Nutrition 59 (2019) 50–55

Contents lists available at ScienceDirect

Nutrition

journal homepage: www.nutritionjrnl.com

Applied nutritional investigation

Body composition evaluation with computed tomography: Contrast media and slice thickness cause methodological errors

Fabian Morsbach M.D. [a,*], Yi-Hua Zhang M.D. [a], Lena Martin R.D., Ph.D. [b], Catarina Lindqvist R.D. [c], Torkel Brismar M.D., Ph.D. [a]

[a] Division of Radiology, Department of Clinical Science, Intervention and Technology, Karolinska Institutet, Karolinska University Hospital, Stockholm, Sweden
[b] Institute of Bioscience and Nutrition, Karolinska Institutet, Karolinska University Hospital, Stockholm, Sweden
[c] Function Area Clinical Nutrition, Department of Medicine, Karolinska Institutet, Karolinska University Hospital, Stockholm, Sweden

ARTICLE INFO

Article History:
Received 21 April 2018
Received in revised form 11 July 2018
Accepted 3 August 2018

Keywords:
Skeletal muscle index
Muscle
Fat
Segmentation
Computed tomography
Body composition

ABSTRACT

Objective: Although computed tomography (CT) is frequently used to determine body composition, the effects of using different CT protocols is not well known. The aim of this study was to determine whether contrast media phase, radiation dose, and slice thickness in CT affect body composition segmentation.
Methods: Clinically indicated perfusion CTs of the upper abdomen in 20 patients (seven women) between 40 and 87 y of age with high suspicion of hepatocellular carcinoma were analyzed retrospectively. Axial images from the L3 level with varying imaging delay were reconstructed after contrast media injection (18 images per patient), slice thickness (5 images, 2–10 mm), and radiation dose (4 images with one-third to four-thirds of standard dose). Muscle and fat areas were segmented semiautomatically by drawing regions of interests and using established cutoff thresholds. Skeletal muscle index (SMI), steatotic muscle area, and adipose tissue index, as well as muscle attenuation and fat attenuation, were evaluated.
Results: Average SMI increased by up to 2.8% after contrast media injection. Steatotic muscle area decreased by ≤13.8%, and adipose tissue index decreased by ≤6.5%. Muscle attenuation increased after contrast media injection, whereas fat attenuation decreased (all $P < 0.001$). SMI decreased by 1.9% on average when increasing slice thickness from 2 to 10 mm. Steatotic muscle area increased by ≤3.3%, and adipose tissue index increased by ≤1.5% (all $P < 0.05$). Muscle attenuation did not change significantly with reconstruction thickness. Radiation dose had no effect on estimated area of spinal muscle, fatty spinal muscle, or visceral fat.
Conclusions: Contrast media have a strong effect on the evaluation of body composition, whereas the influence of slice thickness is less pronounced. Radiation dose can be reduced by ≥66% without significantly affecting segmentation.

© 2018 Elsevier Inc. All rights reserved.

Introduction

The first analyses of body composition were used for analyzing muscle loss in astronauts or for evaluating dietary regimens in obese patients [1]; however, during recent decades body analyses have gained increasing interest when evaluating cancer cachexia [2] and critically ill patients [3]. Initial methodology was based on dual-energy x-ray absorptiometry (DXA), underwater weighing, and bioimpedance [4]. These techniques, however, could not distinguish between muscle groups or between subcutaneous and intraabdominal fat. It was shown early that computed tomography (CT) [5] could be used for such discrimination, but at the cost of ionizing radiation. To avoid radiation and to enable whole-body analyses in large population groups, techniques based on magnetic resonance imaging (MRI) have been developed [6,7]. However, CT is more likely to be readily available for hospitalized patients.

For research on clinical materials, CT is increasingly used to determine body composition and, together with DXA and MRI, is considered the standard of reference for body composition measurements [8,9]. CTs for clinical purposes (i.e., when evaluating cancer treatment or suspected complications in critically ill patients) [10,11], often are analyzed retrospectively to study body composition. Those scans most often include the abdomen [10,11], which makes it easy to perform body composition analysis. Concerning

The authors all participated sufficiently in the work to take public responsibility for the content, including participation in the concept, design, analysis, writing, or revision of the manuscript. FM is supported by a grant by the Helmut-Hartweg-Fonds from the Swiss Academies of Arts and Sciences and the Swiss Radiologic Society. YHZ is the recipient of AT-funding from Karolinska Institutet. The authors have no conflict of interest to declare.

* Corresponding author: Tel.: +46 734 55956; Fax: +46 8 585 84692.
E-mail address: Morsbachfabian@gmail.com (F. Morsbach).

https://doi.org/10.1016/j.nut.2018.08.001
0899-9007/© 2018 Elsevier Inc. All rights reserved.

cachexia in patients with cancer in particular, body segmentation has been shown to be of value in evaluating progressive loss of muscle mass [11,12]. Many researchers are studying muscle mass in patients with liver cirrhosis and its association with mortality [13–15]. Moreover, CT has been suggested as the preferred method for analyzing muscle quality to determine sarcopenia, but standardized CT parameters have not been defined [11,16]. However, CT segmentation has mainly been validated on unenhanced CT scans and cadavers [5,17], and clinical CT scans may or may not be performed with contrast enhancement [11]. Many studies do not report the details of CT methodology, such as tube potential (kV), slice thickness, or whether contrast media were used [12,14,18]. This might be due to lack of knowledge of the effect of different CT acquisition parameters on body composition segmentation. Recent radiologic recommendations to use lower tube potential to reduce radiation and contrast media dose will complicate matters further because the attenuation values of the tissue change with tube potential [19].

The purpose of this study was to determine whether changes in the CT's contrast media phase parameters, radiation dose, and slice thickness have an effect on body composition segmentation.

Material and methods

Patient population

This retrospective study analyzed clinically indicated perfusion CTs of the upper abdomen in 20 patients (7 women) between 40 and 87 y of age with high suspicion of hepatocellular carcinoma. Mean body mass index was 21.2 kg/cm^2 (range 15.2–24.2 kg/cm^2). Inclusion criteria were a perfusion CT with at least four unenhanced series, no severe motion artifacts, and inclusion of the abdomen at the level of the L3 vertebra [20].

This study was approved by the local ethics committee and written informed consent was given.

Perfusion CT

At perfusion CT imaging, the inflow of contrast media is "filmed" by performing repeated low-dose scans. These scans are typically performed at intervals of 1.5 to 3 s. Perfusion imaging gives information on the arterialization of the tumor and the surrounding tissue. In this study, all patients were examined with a second-generation 128-slice dual-source CT system with stellar detectors (Somatom Definition Flash, Siemens Healthcare, Forchheim, Germany). Images were acquired with a 4-dimensional (4-D) dynamic spiral CT mode with variable pitch [21]. The target volume was fixed at 14.8 cm in the z axis and defined on the topogram to include the upper abdomen. Contrast medium application included 60 mL of iodine-containing contrast medium (Iomeron, 400 mg iodine/mL; Bracco Diagnostics Inc., Princeton, NJ, USA), which was injected through an 18-gauge needle into an antecubital vein at a flow rate of 7 mL/s followed by 50 mL of saline solution at the same flow rate. The resulting injection time was 8.5 s. Imaging was initiated after an 8-s delay to allow acquisition of baseline unenhanced images. Twenty-seven acquisitions were obtained using the dynamic spiral acquisition mode with variable pitch during a total examination time of 54 s. This resulted in 27 separate series that can be used for further evaluation. The images were acquired continuously in consecutive craniocaudal/caudocranial directions by accelerating the table to a pitch value of 0.75 and decelerating to a full stop with an acquisition time of 2 s for each direction (cycle time, 2 s). Each examination was performed with free shallow breathing. Further imaging parameters were 80 kV tube voltage, 160 mAs tube current-time product, 0.20-s gantry rotation time and 128 × 0.6-mm slice collimation. The radiation dose of each of the 27 series was approximately equal to 33% of a standard CT [22].

Image postprocessing

Images were reconstructed with a standard filtered back-projection with a medium smooth tissue kernel (B20 f) [21]. For every time point, a single series was reconstructed with a slice thickness of 1.5 mm and an increment of 1 mm, resulting in 27 series. This resulted in at least four unenhanced series, with subsequent arterial and early portal venous phases. All images were transferred to a Syngo.via Server (Syngo.via VB10 B, Siemens Healthcare, Forchheim, Germany) for further postprocessing. All split series were loaded into the perfusion application. Motion correction and 4-D noise reduction were applied [23].

Image reconstruction for analysis of contrast media influence

After analysis of the time-attenuation curve derived from the aorta, images were arranged in four unenhanced series, 12 consecutive series after the enhancement in aorta reached a threshold of 100 HU (acquisition of images ~20 s after reaching the threshold are deemed "arterial phase"), and two early portal venous phases defined as the last two series of the acquisition (Fig. 1). From each series, a single image was reconstructed in the axial plane with a slice thickness of 5 mm at the level of L3, resulting in 18 images for analysis with varying contrast media influence obtained from each patient.

The four unenhanced series were used to create average intensity projections combining up to four time points. This resulted in four reconstructed series with increasing theoretical radiation dose from 1/3 to 4/3 of the regular dose [24]. From each series, a single image was reconstructed in the axial plane with a slice thickness of 5 mm at the level of L3 matching the same level on the z axis as in the time-resolved reconstructions. Thus, four images with increasing theoretical radiation dose were obtained from each patient for analysis.

Image reconstruction for analysis of slice thickness influence

Three time points from the unenhanced series were averaged, and images with a slice thickness of 2, 3, 4, 5, and 10 mm were reconstructed. Similar to the analysis of contrast media and radiation dose influence, axial images were selected at the level of L3. Thus, five images with increasing slice thickness were obtained from each patient.

In all, for the analysis of contrast media dose, radiation dose and slice thickness, 27 images at the L3 level were obtained per patient resulting in 540 images to analyze.

Image analysis

The images at L3 level were segmented using established thresholds: area of muscle, −29 to 150 HU; hypoattenuating/steatotic muscle, −29 to 30 HU; fat −150 to −30 HU. The psoas and paraspinal muscles (erector spinae, quadratus lumborum), abdominal wall muscles (transversus abdominus, external and internal obliques, rectus abdominus), visceral adipose tissues, and subcutaneous adipose tissues were manually segmented using the freely available software ImageJ (https://imagej.nih.gov/ij/download.html, Fig. 2) by a radiologist (with >5 y experience in body imaging). Total area in cm^2 and mean attenuation (HU) were recorded for each segmented region. At the contrast media dose analysis, a region of interest was also placed in the aorta to determine the point at which the threshold of 100 HU was met.

For further analysis, the skeletal muscle mass area at L3 (in cm^2) was normalized for height (cm^2/m^2) to calculate SMI [18]. The area of steatotic muscle at L3 (cm^2) was analyzed. The area of adipose tissue at L3 was normalized for height (cm^2/m^2) to calculate adipose tissue index.

Statistical analysis

Normality was determined by the Kolmogorov–Smirnoff test. To detect differences between segmentation results, repeated measures analysis of variance was used. Bonferroni adjustments for confidence intervals were applied. Post hoc testing was performed with Student's *t* test for paired samples.

Mean difference was calculated between different reconstruction series and is presented in percent. Data were analyzed using commercially available software (IBM SPSS Statistics for Windows, Version 22.0. Armonk, NY, USA: IBM Corp and R Foundation for Statistical Computing, Version 3.2.1, Vienna, Austria). A two-tailed $P < 0.05$ was considered statistically significant.

Results

Influence of contrast enhancement

SMI, muscle attenuation, steatotic muscle area, adipose tissue index, and fat attenuation all showed significant overall differences related to contrast enhancement (all $P < 0.001$; Table 1). SMI increased over time after contrast media injection, whereas steatotic muscle area and adipose tissue index decreased after contrast application. The maximum mean increase of SMI was 2.8% between the last acquired contrast-enhanced scan (equaling an early portal venous phase) and unenhanced scan ($P < 0.001$). The corresponding decrease of steatotic muscle area was −13.8% ($P = 0.003$; Fig. 3) and that of adipose tissue index was −6.5% ($P < 0.001$).

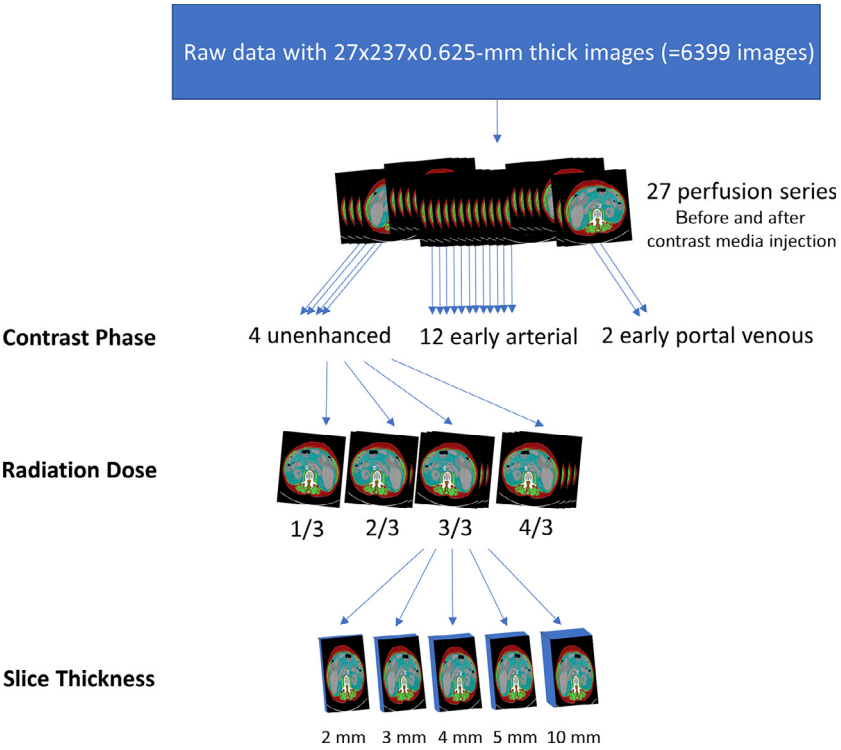

Fig. 1. Flowchart depicting the different reconstructions produced from perfusion computed tomography. Image reconstruction for analysis of radiation dose influence.

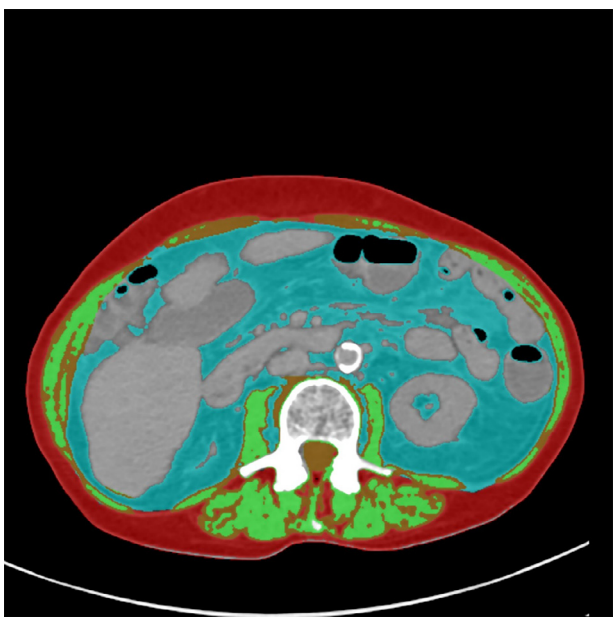

Fig. 2. A segmented axial computed tomography image obtained at the level of the third lumbar vertebra. Subcutaneous adipose tissue (red), visceral adipose tissue (blue), skeletal muscle (green), and steatotic skeletal muscle (brown).

The overall quantified attenuation differed for muscle and fat tissue with respect to contrast enhancement ($P < 0.001$, both). The increase between the early portal venous scan and unenhanced scans for mean spinal muscle density was from 30 to 36 HU ($P < 0.001$; Fig. 4) and for visceral fat, from −90 to −87 HU ($P < 0.001$).

Influence of slice thickness reconstruction

There were significant overall differences for SMI ($P = 0.01$), steatotic muscle area ($P = 0.002$), and adipose tissue index ($P = 0.02$; Table 2). The maximum mean difference was 1.9% ($P = 0.03$) for SMI, 3.3% for steatotic muscle area ($P = 0.02$), and 1.5% for adipose tissue index (95% confidence interval [CI], 0.3%–3.2%; $P = 0.02$). There were no significant differences in attenuation between the five different reconstruction slice thicknesses for muscle tissue ($P = 0.07$, both), whereas the measured density of fat increased from −91 HU at 2 mm to −86 HU at 10 mm ($P < 0.001$).

Influence of radiation dose

There were no significant overall differences for SMI, muscle attenuation, steatotic muscle area, adipose tissue index, or fat attenuation as a function of radiation dose (all $P > 0.05$; Table 3).

Discussion

When analyzing body composition from CT images, the use of contrast media enhancement and the choice of slice thickness have a significant effect on the segmentation results. It is therefore important to keep them constant when evaluating longitudinal changes in clinical cohorts and to be aware of their effect when comparing results between different cohorts. The steatotic muscle area measurements are particularly vulnerable to changes in contrast media phase, where the segmented area was 13.8% smaller on average in the contrast-enhanced series than in the unenhanced series. Also, measurements of fat showed major changes related to contrast media phase, with underestimations of 6.5% during the early portal venous phase. The SMI parameter was less vulnerable,

Table 1
Influence of contrast enhancement on segmentation outcome

Enhancement in the aorta (HU)/Equivalent contrast phase	48/Unenhanced (95% CI)	480/Arterial (95% CI)	168/Early portalvenous (95% CI)	*P*- value
SMI (cm/m^2)	50.1 (45.1–54.9)	51.4 (46.5–56.2)	51.5 (46.7–56.3)	<0.001
Muscle attenuation (HU)	30 (26–35)	35 (30–40)	36 (31–42)	<0.001
Steatotic muscle area (cm^2)	27.2 (21.5–32.9)	24.3 (18.7–30)	24.1 (18.4–29.7)	<0.001
Adipose tissue index (cm/m^2)	147.9 (122.7–173)	138.3 (113.5–163)	138.4 (113.3–163.5)	<0.001
Fat attenuation (HU)	−90 (−96 to −85)	−88 (−94 to −82)	−87 (−93 to −81)	<0.001

HU, Hounsfield unit; SMI, skeletal muscle index
Values presented as mean. Full table available in the addendum

with a more modest overestimation of nearly 3% after contrast enhancement. All these changes can be attributed to the presence of iodine from the contrast media in the tissue. Iodine increases the attenuation of the photons and thereby causes a misclassification of the tissue, skewing it to tissues of higher density than in segmented images obtained without the use of contrast media. Importantly, classification of muscle quality can be affected when contrast media are applied. As shown in the present study, mean muscle tissue attenuation can change significantly. This causes a systematic misclassification when evaluating myosteatosis in patients. The study patient group had an overall low muscle attenuation, averaging 30 HU without contrast media. This is most likely due to the patient group consisting exclusively of patients with liver disease, who are predisposed to myosteatosis [14]. Moreover, the scans were obtained at a low tube potential (80 kV), which also causes changes in attenuation. However, after contrast media application, average attenuation increased to 36 HU. In regard to current recommendations, this change could be relevant in the classification of myosteatosis in patients [11]. The present results confirmed initial findings that the use of contrast media causes a methodological error that overestimates skeletal muscle mass area and average muscle attenuation [25,26]. This highlights the need for standardized CT protocols for body composition evaluation. In comparison with van der Werf's study, the present study showed the influence of contrast media on steatotic muscle area, as well as on fat [25]. The lack of difference in estimated areas and mean attenuation between the four time points obtained before contrast media also shows that possible fluid redistribution does not affect measurements during the scanning period.

Slice thickness also had an effect on segmentation. It was most pronounced when evaluating steatotic muscle area, where increasing attenuation values and decreasing area were obtained when slice thickness was increased. This is because the averaging of pixels from adjacent slices resulted in low values being averaged out by denser areas (e.g., due to small volumes of fat being merged with small volumes of muscle), which increased the average density to above the cutoff level.

Unlike contrast media and slice thickness, radiation dose did not influence the quantified area of SMI, steatotic muscle area, adipose tissue index, or muscle attenuation. This is an important finding as it indicates that radiation dose can be reduced significantly when the sole purpose of the CT is to evaluate body composition.

To avoid misinterpretation of steatotic muscle/myosteatosis and fat in prospective clinical trials, unenhanced series should be measured. Performing further series for research or for clinical evaluation of nutritional status will expose patients to additional radiation. However, this study shows that the radiation dose of such scans can be reduced to at least one-third of the standard dose without affecting the segmentation. If the scan length is limited to 2 to 3 cm the resulting radiation dose will be ~1/30th of an abdominal scan, or ~0.2 mSv, which is equivalent to that of a chest radiograph [22].

The present study had certain limitations, the major limitation being that we used only 60 mL of contrast media, a dose that was fixed for all patients undergoing perfusion CT. Mostly, contrast media are adjusted to body weight [27], resulting in contrast media doses of ≤200 mL. The underestimations of SMI and adipose tissue index after just 60 mL of contrast media in the present study would most probably have been even greater if standard clinical doses of contrast media had been used. Another limitation was that only series from the early portal

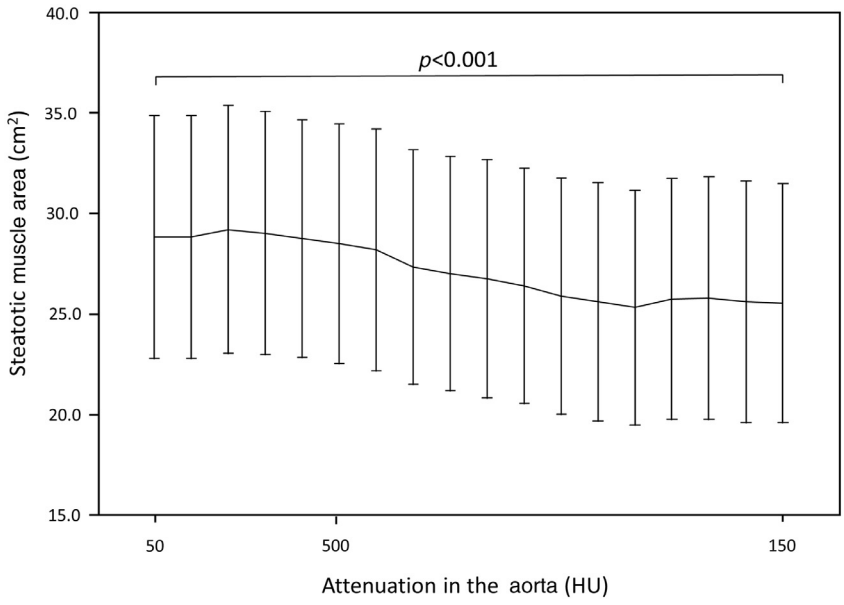

Fig. 3. Line plot of the mean steatotic muscle area measured with different contrast media enhancement time points (whiskers represent 95% confidence intervals).

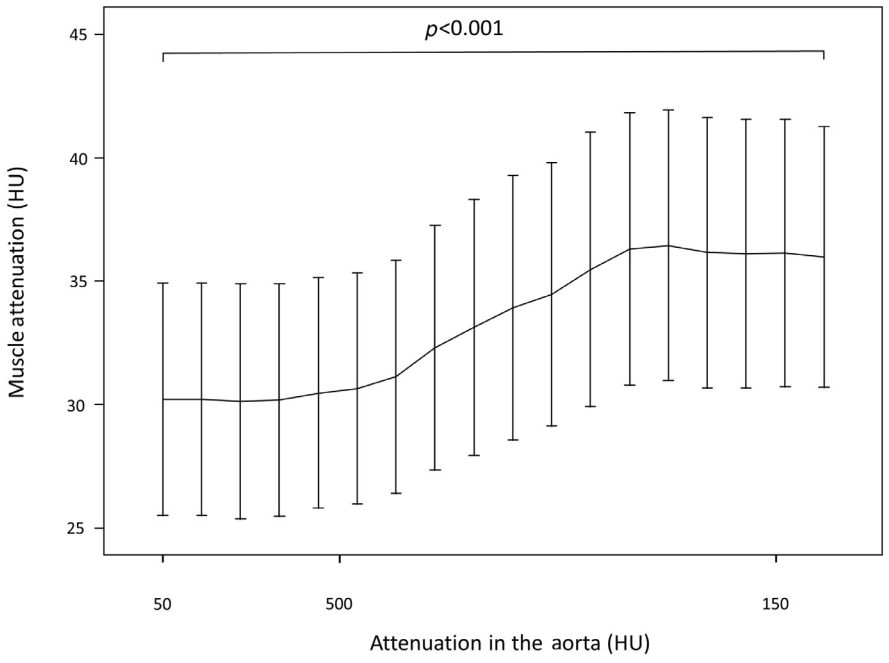

Fig. 4. Line plot of the mean muscle attenuation measured with different contrast media enhancement time points (whiskers represent 95% confidence intervals).

Table 2
Influence of slice thickness on segmentation outcome

Slice thickness (mm)	2 (95% CI)	3 (95% CI)	4 (95% CI)	5 (95% CI)	10 (95% CI)	*P*-value
SMI (cm^2/m^2)	50.5 (45.6–55.4)	50.5 (45.6–55.3)	50.3 (45.4–55.2)	50.1 (45.1–54.9)	49.5 (44.6–54.5)	0.01
Muscle attenuation (HU)	31 (26–35)	30 (26–35)	30 (25–5)	30 (25–35)	30 (25–34)	0.07
Steatotic muscle area (cm^2)	27.2 (21.5–32.9)	27.3 (21.5–33)	27.3 (21.5–33.1)	27.4 (21.6–33.2)	28.1 (22.1–34.1)	0.002
Adipose tissue index (cm^2/m^2)	147.2 (122.1–172.4)	147.6 (122.3–172.9)	147.8 (122.7–173)	147.2 (122.2–172.3)	149 (123.4–174.7)	0.02
Fat Attenuation (HU)	−91 (−96 to −85)	−90 (−96 to −85)	−90 (−95 to −84)	−91 (−97 to −85)	−86 (−91 to −81)	<0.001

HU, Hounsfield unit; SMI, skeletal muscle index
Values are presented as mean.
Every second column omitted for illustration purposes. Full table available in the addendum.

venous phase were available. This was due to tight constraints in the duration of our perfusion CT method designed to limit the already high radiation dose associated with perfusion CT. However, fast injection times in perfusion CT result in earlier portal venous phases [28]. Third, the weight range of the patients was limited, with no severely obese patients. This was because the majority of the patients had liver cirrhosis, which affected their nutritional status. It is probable that the relative influence of contrast media on patients with very large amounts of visceral fat would have been less pronounced, but otherwise the findings should be applicable to very obese patients as well. Another limitation was that radiation dose was calculated from summation of several single time-point perfusion scans, which could differ slightly from separate single abdominal scans due to small differences in scanner parameters. However, such eventual differences should not affect the relative changes in contrast enhancement of the tissues.

Conclusion

Segmentation of body composition varies significantly for CT examinations when contrast media are applied. It varies also to a lesser degree with slice thickness. The radiation dose can be reduced by 66% without affecting segmentation significantly, indicating that low-dose scans could be used in prospective studies on

Table 3
Influence of radiation dose on segmentation outcome

Radiation dose	1/3 Dose	2/3 Dose	3/3 Dose	4/3 Dose	*P*-value
SMI (cm^2/m^2)	50.1 (45–55)	50 (49.9–55)	50.1 (45.1–54.9)	50.1 (45.1–54.9)	0.31
Muscle attenuation (HU)	30 (26–35)	30 (25–35)	30 (25–35)	30 (25–35)	0.10
Steatotic muscle area (cm^2)	27.6 (21.7–33.5)	27.4 (21.6–33.2)	27.4 (21.5–33.3)	27.6 (21.6–33.7)	0.10
Adipose tissue index (cm^2/m^2)	147.6 (122.4–172.8)	147.2 (122.2–172.3)	147.2 (122.2–172.3)	147.6 (122.1–172.4)	0.09
Fat attenuation (HU)	−90 (−96 to −83)	−90 (−96 to −85)	−91 (−97 to −85)	−90 (−96 to −85)	0.43

HU, Hounsfield unit; SMI, skeletal muscle index
Values are presented as mean.
Every second column omitted for illustration purposes. Full table available in the addendum.

body composition. Results from the present study highlighted the importance of using a standardized methodology when comparing body composition analysis in different populations.

Supplementary data

Supplementary data related to this article can be found at https://doi.org/10.1016/j.nut.2018.08.001.

References

[1] Vanderveen JE, Allen TH. Energy requirements of man living in a weightless environment. Life Sci Space Res 1972;10:105–12.
[2] Ryan AM, Power DG, Daly L, Cushen SJ, Ni Bhuachalla E, Prado CM. Cancer-associated malnutrition, cachexia and sarcopenia: the skeleton in the hospital closet 40 years later. Proc Nutr Soc 2016;75:199–211.
[3] Paris M, Mourtzakis M. Assessment of skeletal muscle mass in critically ill patients: considerations for the utility of computed tomography imaging and ultrasonography. Curr Opin Clin Nutr Metab Care 2016;19:125–30.
[4] Heymsfield SB, Gonzalez MC, Lu J, Jia G, Zheng J. Skeletal muscle mass and quality: evolution of modern measurement concepts in the context of sarcopenia. Proc Nutr Soc 2015;74:355–66.
[5] Rossner S, Bo WJ, Hiltbrandt E, Hinson W, Karstaedt N, Santago P, et al. Adipose tissue determinations in cadavers—a comparison between cross-sectional planimetry and computed tomography. Int J Obes 1990;14:893–902.
[6] Karlsson A, Rosander J, Romu T, Tallberg J, Gronqvist A, Borga M, et al. Automatic and quantitative assessment of regional muscle volume by multi-atlas segmentation using whole-body water-fat MRI. J Magn Reson Imaging 2015;41:1558–69.
[7] Levelt E, Pavlides M, Banerjee R, Mahmod M, Kelly C, Sellwood J, et al. Ectopic and visceral fat deposition in lean and obese patients with type 2 diabetes. J Am Coll Cardiol 2016;68:53–63.
[8] Mazonakis M, Damilakis J. Computed tomography: what and how does it measure? Eur J Radiol 2016;85:1499–504.
[9] Mattsson S, Thomas BJ. Development of methods for body composition studies. Physics in medicine and biology 2006;51:R203–28.
[10] Agustsson T, Wikrantz P, Ryden M, Brismar T, Isaksson B. Adipose tissue volume is decreased in recently diagnosed cancer patients with cachexia. Nutrition 2012;28:851–5.
[11] Martin L, Birdsell L, Macdonald N, Reiman T, Clandinin MT, McCargar LJ, et al. Cancer cachexia in the age of obesity: skeletal muscle depletion is a powerful prognostic factor, independent of body mass index. J Clin Oncol 2013;31:1539–47.
[12] Anandavadivelan P, Brismar TB, Nilsson M, Johar AM, Martin L. Sarcopenic obesity: a probable risk factor for dose limiting toxicity during neo-adjuvant chemotherapy in oesophageal cancer patients. Clin Nutr 2016;35:724–30.
[13] Hanai T, Shiraki M, Nishimura K, Ohnishi S, Imai K, Suetsugu A, et al. Sarcopenia impairs prognosis of patients with liver cirrhosis. Nutrition 2015;31:193–9.
[14] Montano-Loza AJ, Angulo P, Meza-Junco J, Prado CM, Sawyer MB, Beaumont C, et al. Sarcopenic obesity and myosteatosis are associated with higher mortality in patients with cirrhosis. J Cachexia Sarcopenia Muscle 2016;7:126–35.
[15] Kalafateli M, Mantzoukis K, Yau YC, Mohammad AO, Arora S, Rodrigues S, et al. Malnutrition and sarcopenia predict post-liver transplantation outcomes independently of the Model for End-stage Liver Disease score. J Cachexia Sarcopenia Muscle 2017;8:113–21.
[16] Fearon K, Strasser F, Anker SD, Bosaeus I, Bruera E, Fainsinger RL, et al. Definition and classification of cancer cachexia: an international consensus. Lancet Oncol 2011;12:489–95.
[17] Mitsiopoulos N, Baumgartner RN, Heymsfield SB, Lyons W, Gallagher D, Ross R. Cadaver validation of skeletal muscle measurement by magnetic resonance imaging and computerized tomography. J Appl Physiol 1998;85:115–22.
[18] Mourtzakis M, Prado CM, Lieffers JR, Reiman T, McCargar LJ, Baracos VE. A practical and precise approach to quantification of body composition in cancer patients using computed tomography images acquired during routine care. Appl Physiol Nutr Metab 2008;33:997–1006.
[19] Seyal AR, Arslanoglu A, Abboud SF, Sahin A, Horowitz JM, Yaghmai V. CT of the abdomen with reduced tube voltage in adults: a practical approach. Radiographics 2015;35:1922–39.
[20] Tong Y, Udupa JK, Torigian DA. Optimization of abdominal fat quantification on CT imaging through use of standardized anatomic space: a novel approach. Med Phys 2014;41:063501.
[21] Goetti R, Leschka S, Desbiolles L, Klotz E, Samaras P, von Boehmer L, et al. Quantitative computed tomography liver perfusion imaging using dynamic spiral scanning with variable pitch: feasibility and initial results in patients with cancer metastases. Invest Radiol 2010;45:419–26.
[22] Ware DE, Huda W, Mergo PJ, Litwiller AL. Radiation effective doses to patients undergoing abdominal CT examinations. Radiology 1999;210:645–50.
[23] Seifarth H, Raupach R, Schaller S, Fallenberg EM, Flohr T, Heindel W, et al. Assessment of coronary artery stents using 16-slice MDCT angiography: evaluation of a dedicated reconstruction kernel and a noise reduction filter. Eur Radiol 2005;15:721–6.
[24] Fischer MA, Leidner B, Kartalis N, Svensson A, Aspelin P, Albiin N, et al. Time-resolved computed tomography of the liver: retrospective, multi-phase image reconstruction derived from volumetric perfusion imaging. Eur Radiol 2014;24:151–61.
[25] van der Werf A, Dekker IM, Meijerink MR, Wierdsma NJ, de van der Schueren MAE, Langius JAE. Skeletal muscle analyses: agreement between non-contrast and contrast CT scan measurements of skeletal muscle area and mean muscle attenuation. Clin Physiol Funct Imaging 2018;38:366–72.
[26] van Vugt JLA, Coebergh van den Braak RRJ, Schippers HJW, Veen KM, Levolger S, de Bruin RWF, et al. Contrast-enhancement influences skeletal muscle density, but not skeletal muscle mass, measurements on computed tomography [Epub ahead of print]. Clin Nutr 2017.
[27] Bae KT. Intravenous contrast medium administration and scan timing at CT: considerations and approaches. Radiology 2010;256:32–61.
[28] Klotz E, Haberland U, Glatting G, Schoenberg SO, Fink C, Attenberger U, et al. Technical prerequisites and imaging protocols for CT perfusion imaging in oncology. Eur J Radiol 2015;84:2359–67.